Frequency equation and semi-empirical mechanical coupling strength of microcantilevers in an array

Dat, L. T., Pham, V. N. T., Vy, N. D., & Payam, A. F. (2022). Frequency equation and semi-empirical mechanical coupling strength of microcantilevers in an array. *Microscopy Research and Technique*, *85*(9), 3237-3244. https://doi.org/10.1002/jemt.24180

Published in:
Microscopy Research and Technique

Publication Status:
Published (in print/issue): 01/09/2022

DOI:
10.1002/jemt.24180

Document Version
Author Accepted version

MICROSCOPY RESEARCH & TECHNIQUE

Frequency equation and semi-empirical mechanical coupling strength of microcantilevers in an array

Journal:	*Microscopy Research and Technique*
Manuscript ID	MRT-22-062
Wiley - Manuscript type:	Research Article
Date Submitted by the Author:	19-Jan-2022
Complete List of Authors:	Dat, Le Tri; Ton Duc Thang University N. T. Pham, Vinh; Ho Chi Minh City University of Education Duy Vy, Nguyen; Van Lang University Payam, Amir F.; Ulster University - Jordanstown Campus
Classifications:	atomic force microscopy < SCANNING PROBE MICROSCOPY
Keywords:	frequency equation, coupling strength, atomic force microscopy, microcantilever, overhang-shaped

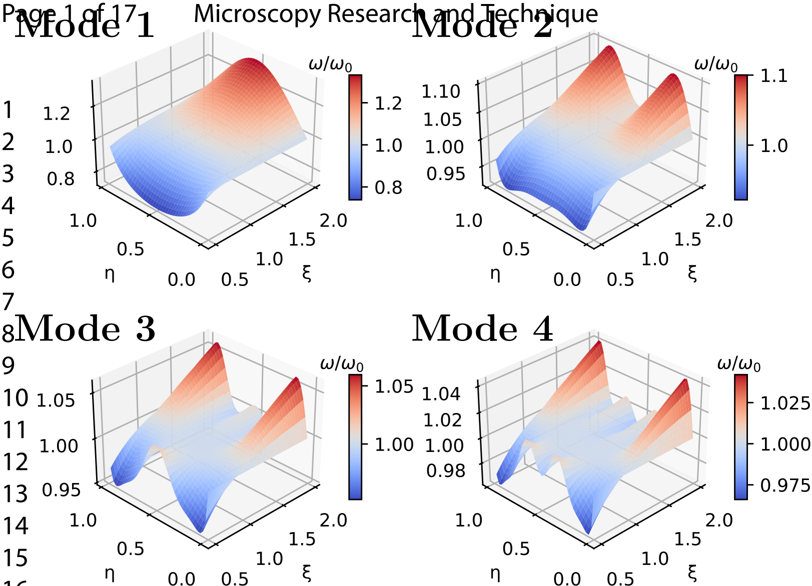
Mode 1
Mode 2
Mode 3
Mode 4
ω/ω0
η
ξ

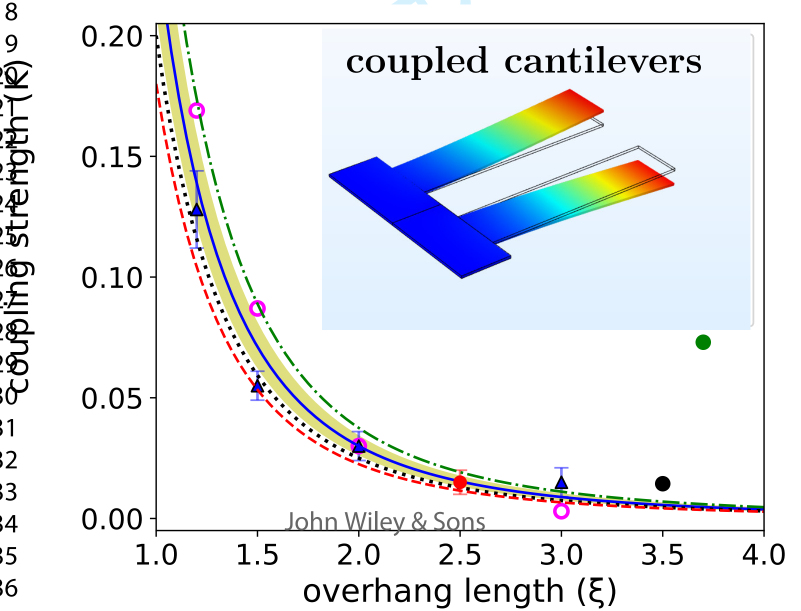
coupled cantilevers
coupling strength (K)
overhang length (ξ)

Highlights:

- A characteristic frequency equation for T- and overhang-shaped cantilevers was derived.
- Mode frequencies and mode gaps could be effectively tuned.
- A formula for coupling strength between cantilevers, was proposed and in good agreement with experimental results and FEM simulation.

Frequency equation and semi-empirical mechanical coupling strength of microcantilevers in an array

Le Tri Dat[1,2,*], Vinh N.T. Pham[3,4], Nguyen Duy Vy[5,6,†], and Amir F. Payam[7,**]

[1]Laboratory of Applied Physics, Advanced Institute of Materials Science, Ton Duc Thang University, Ho Chi Minh City, Vietnam

[2]Faculty of Applied Sciences, Ton Duc Thang University, Ho Chi Minh City, Vietnam

[3]Department of Physics, Hochiminh City University of Education, Ho Chi Minh City, Vietnam

[4]International Cooperation Office, Ho Chi Minh City University of Education, Ho Chi Minh City, Vietnam

[5]Laboratory of Applied Physics, Science and Technology Advanced Institute, Van Lang University, Ho Chi Minh City, Vietnam

[6]Faculty of Technology, Van Lang University, Ho Chi Minh City, Vietnam

[7]School of Engineering, Ulster University, Shore Road, Newtownabbey, Co. Antrim BT37 0QB, United Kingdom

Email: *letridat@tdtu.edu.vn, **a.farokh-payam@ulster.ac.uk

Correspondence: Van Lang University, Ho Chi Minh City, Vietnam

Email: †nguyenduyvy@vlu.edu.vn

Abstract- A characteristic equation for the frequencies of the T-shaped and overhang-shaped cantilevers is derived for the first time. We show that there are optimum values of the overhang lengths and widths that maximize the frequency and the number of maxima is corresponding to the mode number. The frequency of higher-order modes could be tuned by changing the overhang dimensions. Especially, a semi-empirical formula for the coupling strength (κ) between cantilevers in an array is proposed where the strength presents a cubic decrease with the overhang width (ξ) and a linear increase with the overhang length (η), $\kappa = \eta / \xi^3$. There is a very good agreement between the proposed formula and the values obtained in recent experiments by other researchers.

***Keywords*-** frequency equation, coupling strength, microcantilever, AFM, overhang-shaped

1. INTRODUCTION

Microcantilevers are at the heart of a wide range of technology: actuators in MEMS, sensors, energy harvesters, and atomic force microscopy (Huber, Lang, Zhang, Rimoldi, & Gerber, 2015; Kim et al., 2013; Payam, Trewby, & Voïtchovsky, 2018; Sposito, Kurdekar, Zhao, & Hewlett, 2018; Toda, Inomata, Ono, & Voiculescu, 2017; Nguyen Duy Vy, Tri Dat, & Iida, 2016; Xu & Siedlecki, 2009). Recently, microcantilever arrays are widely used to increase the versatility and detecting speed in chemical and bio-sensing (Chen, Huang, & Lai, 2008; Gil-Santos, Ramos, Pini, Calleja, & Tamayo, 2011; McKendry et al., 2002; Plaza et al., 2006). They also present several interesting nonlinear dynamics and physical phenomena such as the collective dynamics (Kimura & Hikihara, 2009; Sato, Hubbard, & Sievers, 2006). The cantilevers could be independently actuated or dependently coupled via electrical (Krylov, Lulinsky, Ilic, & Schneider, 2014), mechanical (Adiga et al., 2009; Cai, Zhang, Wang, Zhao, & Wu, 2013; Chopard, Lacour, & Leblois, 2014; Kimura & Hikihara, 2009; Plaza et al., 2006), or both (Napoli, Wenhua, Turner, & Bamieh, 2005) channels. The coupling between cantilevers is crucial for excitation and controlling the vibration and response of the other cantilevers. Mechanically, it could attribute to a net (Cai et al., 2013) or a full bridge (the overhang, Fig. 1(top)) between subsequent cantilevers (Chopard et al., 2014; Endo, Yabuno, Higashino, Yamamoto, & Matsumoto, 2015; Mukhopadhyay et al., 2005; Spletzer, Raman, Wu, Xu, & Reifenberger, 2006; Yabuno, Seo, & Kuroda, 2013). It is the crucial factor in parallel sensing with array; nevertheless, in fabrication of single cantilevers it could be the unexpected sideback because its dimensions and properties are challenging to control.

In a cantilever array, the overhang plays the key role of the coupling mechanism. However, a rigorous study on the dependence of the overhang dimensions on this coupling strength (κ) is still open to question and is usually estimated based on the measurement using various cantilevers. These overhangs could significantly modify the frequency especially for short cantilevers (Guillon et al., 2011) and transduce the dynamics of the excitation. Therefore, analyzing the properties of the overhang, such as its effect on the final frequency of the cantilever, is of interest. Many efforts have been performed to examine the width-varying cantilevers involving overhang-, trapezoid-, or T-shaped cantilevers. For example, by assuming an analytical function for varying widths, one could obtain a frequency equation (Singh, Pal, & Pandey, 2015); however, it is usually lengthy and complicated.

In general, the frequency (and the modeshapes) is determined from a characteristic frequency equation. For overhang cantilevers, such an equation has not been figured out and the authors usually come with an approximation or numerical results by finite element method (FEM) simulation. In these approximations, the mode shape is assumed to be the ideal form of a rectangular cantilever and the Rayleigh's energy method is adopted. However, this method is correct only if the mode shape is correct (Blevins, 2015; Tamayo, Ramos, Mertens, & Calleja, 2006), which has been skipped in several studies. In fact, in a recent study where the deformation is approximate, it has been shown that if mode shapes satisfy only some boundary conditions, one could obtain some results on the frequency (Meirovitch, 1967).

In this study, we theoretically figure out the frequency equation for the microcantilever with an overhanging part based on the Euler-Bernoulli beam theory. Dependence of the cantilever frequency on the overhang width and length will be revealed. The analytical results are then confirmed with that from the FEM simulation which shows a low relative deviation between the two calculations, below 3%. Especially, a semi-empirical coupling strength (κ) between cantilevers has been proposed which presents a cubic decay with the cantilever's distance (~ overhang width ξ) and a linear increase with the overhang length (η) according to the rule $\kappa = \eta / \xi^3$. A comparison to the experimental values has been performed and a good agreement was obtained.

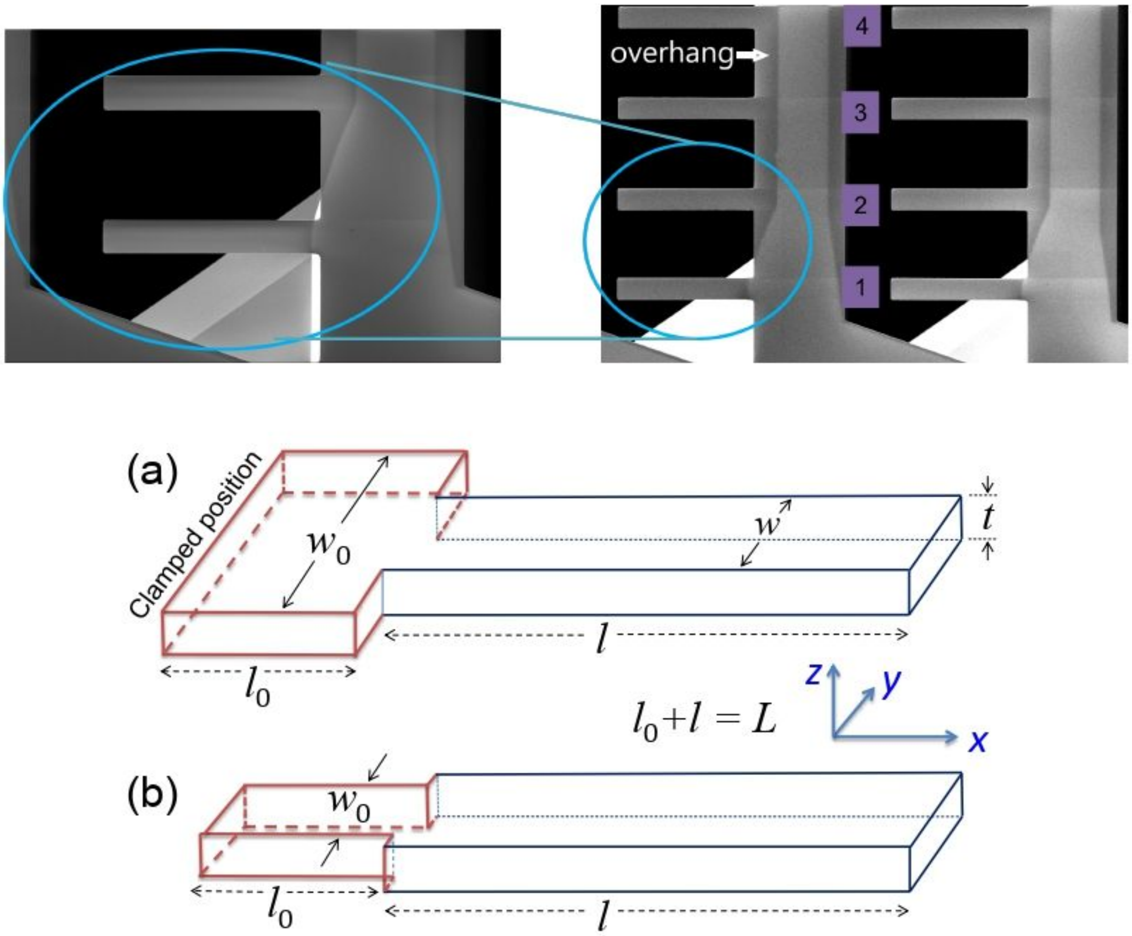

Figure 1: SEM image of the cantilevers without (1) and with (2,3, and 4) overhangs. (a) A model for a microcantilever (width w and length l) with an overhanging part of length l_0 and width $w_0 > w$. The thickness is assumed to be uniform, t, and the total length is $L = l_0 + l$. (b) A T-shaped cantilever with $w_0 < w$. Throughout the paper, the reduced dimensions $\xi = w_0 / w$ and $\eta = l_0 / L$ are frequently used.

2. CHARACTERISTIC FREQUENCY EQUATION

A cantilever with overhang of a same thickness (t) is modeled in Fig. 1(a). The overhang (length l_0 and width w_0) locates between the main cantilever (length l and width $w < w_0$) and the (clamped) fixed base. If $w_0 < w$, one has a T-shaped cantilever [Fig. 1(b)]. The Euler-Bernoulli beam theory is used to study the frequency and mode shapes of the cantilever. The dynamic equation is written as

$$m(x)\frac{\partial^2 V(x,t)}{\partial t^2} = -\frac{\partial^2}{\partial x^2}\left[EI(x)\frac{\partial^2 V(x,t)}{\partial x^2}\right], \tag{1}$$

where, the deflection $V(x,t)$ is a function of position x and time t, $m(x)$ is the mass per unit length. E and $I(x)$ are the (elastic) Young's modulus and the area moment of inertia of cross section, respectively. Using the method of separation of variables, $V(x,t) = W(x)G(t)$, one obtains $G''(t) + \omega^2 G(t) = 0$ and

$$\frac{d^2}{dx^2}\left[EI(x)\frac{d^2 W(x)}{dx^2}\right] - m(x)\omega^2 W(x) = 0. \tag{2}$$

In the case without overhang, $w_0 = w$, and a uniform mechanical property along the length, $I(x)$ is independent on x and Eq. (2) returns to $W^{(4)}(x) - \beta_L W(x) = 0$, where $\beta_L = m\omega^2/(EI)$. Solving this equation using suitable boundary conditions, $W(x)$ is obtained. Especially, a characteristic frequency equation is also revealed,

$$1 + \cos\beta_L L \cosh\beta_L L = 0. \tag{3}$$

This is the famous transcendental equation and its roots are numerically solved (Timoshenko & Young, 1937), $\beta_{L,i}L = 1.875, 4.694, 7.854, 10.995, \ldots$ for i = 1, 2, 3, etc. These $\beta_{L,i}$ determine the frequencies of all singly clamped cantilevers provided that its elastic strength and mass density are known, $\omega_i = \beta_{L,i}^2\sqrt{\frac{EI}{m}}$. Considering the cantilever with an overhang, position-dependent $I(x)$ and $m(x)$ are I_0 and M_0 for $x \le l_0$ and are I and M for $x \ge l_0$, respectively. Then, we have $W_0^{(4)}(x) - \beta_0^4 W_0(x) = 0$ for $0 \le x \le l_0$ and $W^{(4)}(x) - \beta^{(4)} W(x) = 0$ for $l_0 \le x$, where $\beta_0^4 = \frac{M_0\omega^2}{EI_0}$ and $\beta^4 = \frac{M\omega^2}{EI}$; therefore,

$\dfrac{\beta_0}{\beta} = \left(\dfrac{IM_0}{I_0 M}\right)^{1/4} = 1 \Leftrightarrow \beta_0 = \beta$. The solutions of such equations are of the form $W_0(x) = A_1 \sin\beta x + B_1 \cos\beta x + C_1 \sinh\beta x + D_1 \cosh\beta x$, (and similarly, $W(x) = A_2 \sin\beta x + \ldots$). Using $\xi = I_0 / I = w_0 / w$ as the reduced overhang width, we obtain the equation

$$K.X = 0 \tag{4}$$

where $X = \begin{bmatrix} A_1 & B_1 & C_1 & D_1 & A_2 & B_2 & C_2 & D_2 \end{bmatrix}^{\mathrm{T}}$ is a column matrix and K is a square matrix contaning the dimensions of the cantilever and the overhang,

$$K = \begin{bmatrix} 0 & 1 & 0 & 1 & 0 & 0 & 0 & 0 \\ 1 & 0 & 1 & 0 & 0 & 0 & 0 & 0 \\ 0 & 0 & 0 & 0 & -\sin\beta(l_0+l) & -\cos\beta(l_0+l) & \sinh\beta(l_0+l) & \cosh\beta(l_0+l) \\ 0 & 0 & 0 & 0 & -\cos\beta(l_0+l) & \sin\beta(l_0+l) & \cosh\beta(l_0+l) & \sinh\beta(l_0+l) \\ \sin\beta l_0 & \cos\beta l_0 & \sinh\beta l_0 & \cosh\beta l_0 & -\sin\beta l_0 & -\cos\beta l_0 & -\sinh\beta l_0 & -\cosh\beta l_0 \\ \cos\beta l_0 & -\sin\beta l_0 & \cosh\beta l_0 & \sinh\beta l_0 & -\cos\beta l_0 & \sin\beta l_0 & -\cosh\beta l_0 & -\sinh\beta l_0 \\ -\xi\sin\beta l_0 & -\xi\cos\beta l_0 & \xi\sinh\beta l_0 & \xi\cosh\beta l_0 & \sin\beta l_0 & \cos\beta l_0 & -\sinh\beta l_0 & -\cosh\beta l_0 \\ -\xi\cos\beta l_0 & \xi\sin\beta l_0 & \xi\cosh\beta l_0 & \xi\sinh\beta l_0 & \cos\beta l_0 & -\sin\beta l_0 & -\cosh\beta l_0 & -\sinh\beta l_0 \end{bmatrix} \tag{5}$$

Solving this matrix, we obtain

$$2\xi(1+\cos\beta L\cosh\beta L) + (\xi^2-1)(\cos\beta l_0\cosh\beta l_0 + \cos\beta l\cosh\beta l) + (1-\xi)^2(1+\cosh\beta l\cosh\beta l_0\cos\beta l\cos\beta l_0) = 0 \tag{6}$$

Letting $f(x) = \cos\beta x\cosh\beta x$, we arrive with

$$[1+f(L)] + (\xi^2-1)[f(l_0)+f(l)] + (1-\xi)^2[1+f(l_0)f(l)] = 0. \tag{7}$$

This is the characteristic frequency equation for the cantilever with an overhanging part. It maintains the form of Eq. (3) (first term) for a rectangular cantilever and has additional terms symmetric with l_0 and l. Therefore, the eigenvalues for the frequency are functions of l_0 and $\xi = w_0 / w$, $\beta = \beta(l_0, \xi)$. In case without the overhang, $l_0 = 0$, Eq. (7) returns Eq. (3), $1 + f(L) = 0$, when $\beta = \beta_L$. The frequencies with and without overhang are $\omega_i = \beta_i^2 \sqrt{\dfrac{EI}{M}}$ and $\omega_i^0 = \beta_{L,i}^2 \sqrt{\dfrac{EI_{L,w}}{M_{L,w}}}$, respectively. It is worthy to mention that I and M here corresponds to the cantilever part $\{l, w\}$ which could be accurately measured in experiments. Because $I / M = I_0 / M_0$, we have

$$\frac{\omega}{\omega_0} = \frac{\beta^2}{\beta_L^2}. \tag{8}$$

Knowing β, one could directly obtain the resonance frequency. Equation (7) is the new transcendental equation and will be solved by numerical calculations. Let $\eta = l_0 / L$ be the overhang-to-full length ratio, Fig. 2 presents β for the first 4 modes normalized to that of a rectangular cantilever (β_0) of the case the overhang width is $w_0 = w$. The 1st mode [Fig. 2(a)] presents a simple increase of frequency with ξ, or w_0, if $\xi > 1$. At $l_0 = 0$, the cantilever is rectangular of width w and $l = L$. For a certain value of ξ, $\beta_{\eta=0} = \beta_{\eta=1}$ because cantilevers of different widths but a same length will have a same frequency (same I / M ratio). β has one maximum (if $\xi > 1$) and one minimum (if $\xi < 1$) locating at $\eta = 0.5$. Especially, the number of maxima (when $\xi > 1$) is corresponding to the mode number and the change in β with overhang length η is more complicated; however, it is symmetric versus the half length, $0.5L$. For example, the second mode has two maxima, at $\eta = 0.2$ and 0.8. The third mode peaks at 0.1, 0.9, and 0.5 and the fourth mode, at around 0.08, 0.92, 0.35, and 0.65. A cut at $\xi = 1.5$ shown in Fig. 2(e)–(h) makes clear these characteristics. The behavior of T-shaped cantilevers could be seen when $\xi < 1$ [blue region in Fig. 2]. The frequencies of the 1st and 2nd modes are decreased. However, for higher modes, an asymptotical increase of β to β_0 at a certain length is clearly seen. This characteristic could be used to enhance the frequency of higher-order modes.

Table 1: Deviations between analytical and numerical calculation, for $\kappa = 3$, are mostly not greater than 3%.

$\kappa = 3.0$	Mode 3 (kHz)		Deviation (%)	Mode 4 (kHz)		Deviation (%)
η	Analytical	FEM		Analytical	FEM	
0.1	517.18	506.93	-1.98	991.14	980.82	-1.04
0.2	500.60	502.75	0.43	916.33	902.49	-1.51
0.3	462.11	452.93	-1.99	928.85	900.11	-3.09
0.4	469.61	456.52	-2.79	934.94	933.82	-0.12
0.5	484.71	481.75	-0.61	897.59	875.89	-2.42
0.6	469.61	469.75	0.03	934.94	905.92	-3.10
0.7	462.11	450.09	-2.60	928.85	931.00	0.23
0.8	500.60	482.60	-3.60	916.33	888.91	-2.99
0.9	517.18	517.77	0.11	991.14	973.06	-1.82

The analytical calculation could be confirmed using the FEM simulation. Parameters of a Silicon cantilever with $L = 200\ \mu m,\ w = 20\ \mu m,\ t = 0.8 \mu m,\ E = 160$ GPa, and $\rho = m / L = 2320$ kg/m^3, are used. A cut at ξ = 1.5 clearly reveals the dependence of $f = \omega / (2\pi)$ on the overhang length. The deviations are mostly not greater than 0.5% (see the Supplementary Information). Increasing ξ up to 2.5, the deviations below 3% are seen. Increasing w_0, for example ξ > 3, leads to the less accuracy of the assumption that all parts of the overhang deflect as a 1D cantilever. Because while the end part of the overhang (at l_0) deflects with the cantilever, the further part of the shoulder, due to the strong connection with the clamped substrate, receives smaller bending. As a results, the entire cantilever suffers a smaller deflection and a higher frequency in comparison to that from Eq. (7). For the cantilever part $\{l, w\}$, it is clamped by a soft "substrate" $\{l_0, w_0\}$, this is equivalent to an extra effective length l_{eff}. As a results, the frequency of the $1 + l_{eff}$ cantilever is lower than that of the l cantilever, as seen in a recent experiment (Guillon et al., 2011). This explains the higher values from FEM in comparison to the analytical result. Therefore, a 2D analysis should be used if much higher accuracy is required. Nevertheless, in the current 1D calculation, the deviation is mostly less than 3% [see Table I].

Significant change of frequency is presented in Figs. 2(e)–(f) using various cut positions. Especially, it presents an increase of f of the 3rd mode for η = 0.5 [red dashed line, Fig. 2(g)] or of the 4th mode for η = 0.4 [blue dash-dotted line, Fig. 2(h)]. This opens a method for tuning and increasing higher-order resonance frequencies in addition to using an optical resonance cavity shown in a recent study (Hoang, Vy, Dat, & Iida, 2017).

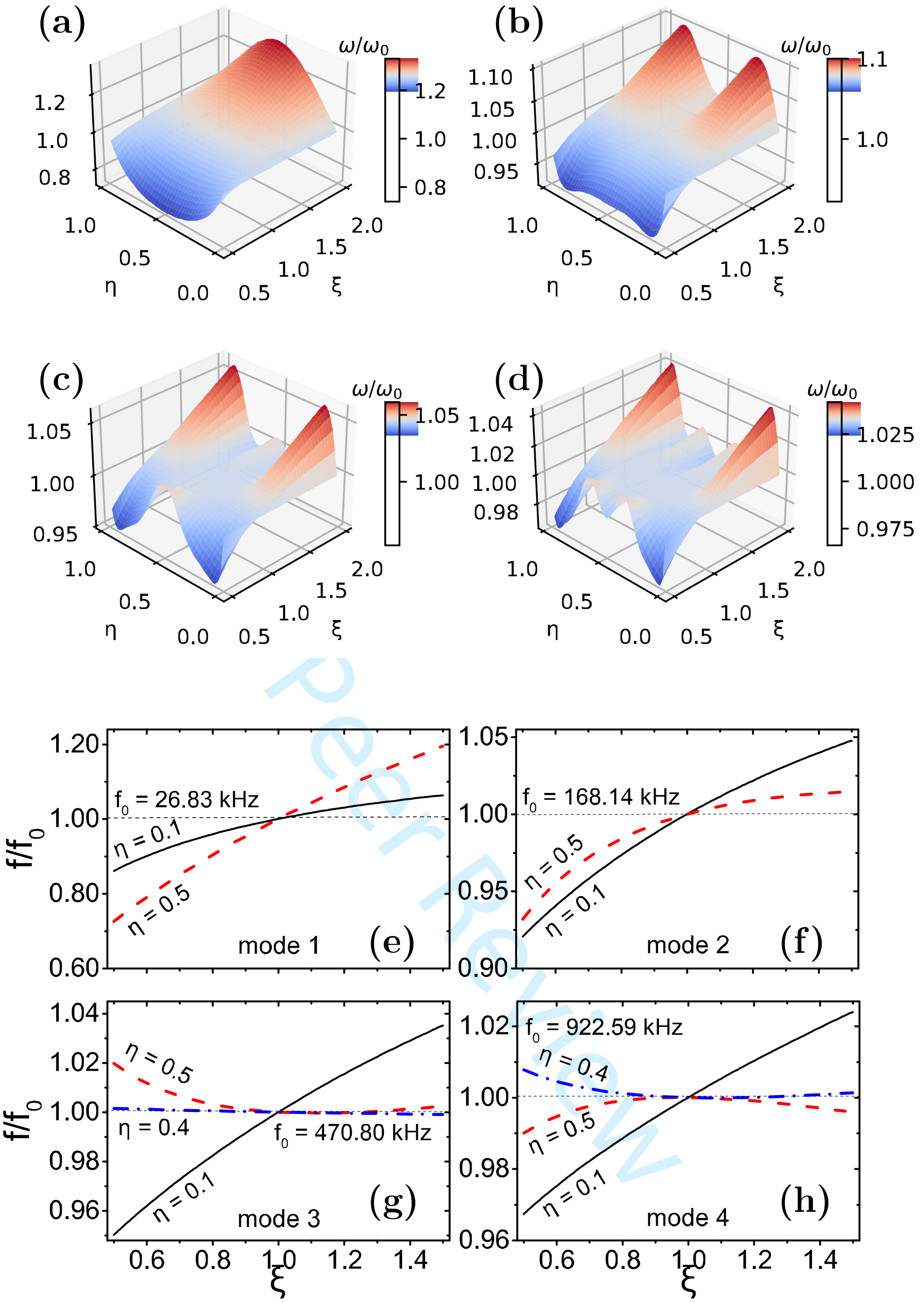

Figure 2: (a)–(d) The frequency ratio (β/β_0) versus the overhang length $\eta = l_0/L$ and width $\xi = w_0/w$ for the first 4 modes. The numbers of maxima (when ξ > 1) is corresponding to the mode number. (e)–(h). Corresponding cuts from (a)–(d) at some values of η reveal the change of frequency versus overhang width. Frequency of the 4th mode in T-shaped cantilever [blue dash-dotted line, ξ < 0.8 (h)] could be increased.

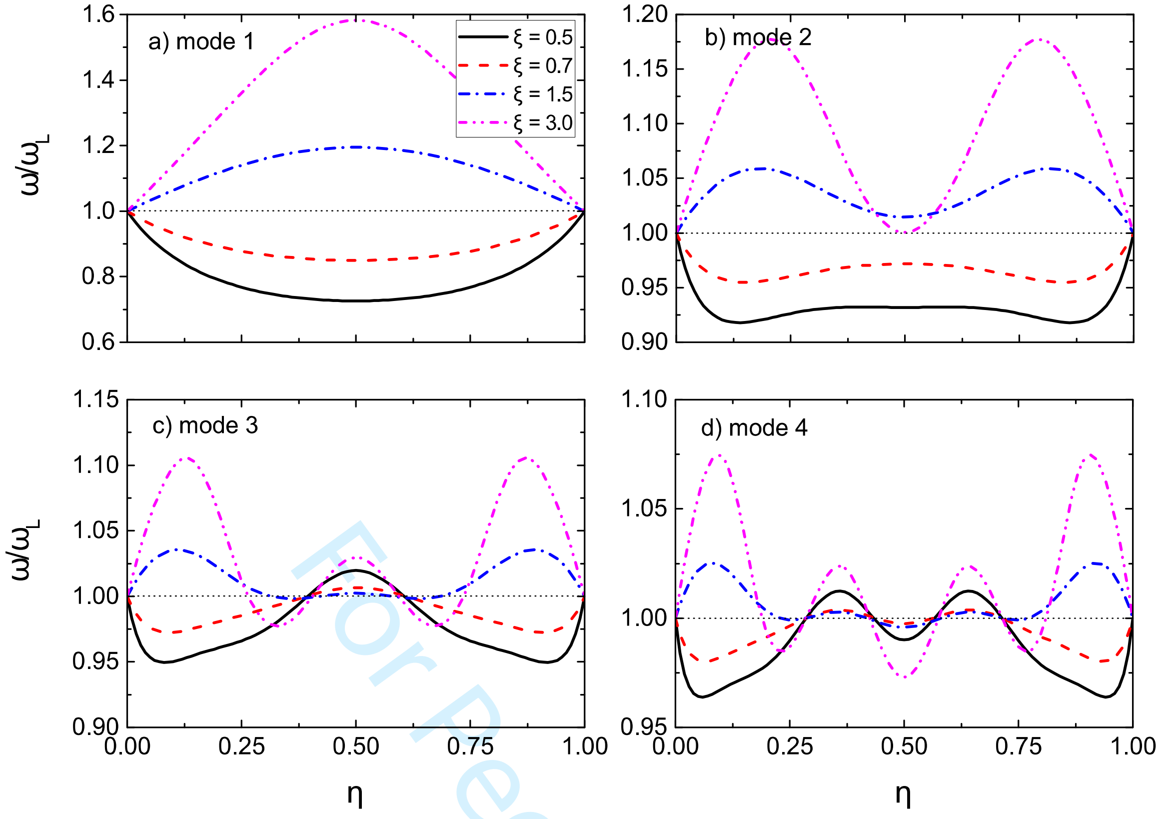

Figure 3: Frequency ratio of the first four modes for various values of ξ. The cantilever frequency could be effectively tuned by changing the internal parameters ξ and η.

Change in frequencies of various modes is significant in measurement, especially when we could bring the modes closer or further, as shown in Fig. 3. Using ξ = 3, for example, while the frequency of the 1st and 2nd modes are increased, the 4th mode, on the other hand, decreased. This behaviour is also seen at other value of ξ. This means the frequency ratio between modes has been effectively alter depending on the internal parameters of the structure. From the physics viewpoint, the change in the boundary conditions inside the cantilever (as a waveguide) gives rise to the change in the eigenvalues of the system. This opens a way to control the relative frequency of the cantilever.

3. THE EFFECT OF NUMBER OF CANTILEVER

Due to the diminishing of oscillation over distance, the effect of the number (n) of nearby cantilevers on the frequency of a single cantilever has been checked, using $\eta = 0.1$ as an example. It is clearly seen in Fig. 4 that the frequency gets an asymptotic value for $n \geq 4$ (violet diamonds) and the asymptotic behaviour is obtained faster for greater cantilevers' distance (ξ). For $\xi \geq 1.2$, the difference in the frequency is negligible for the number $n \geq 2$ (blue triangles). Therefore, we could determine the coupling strength in any array using the results from that of two coupled cantilevers.

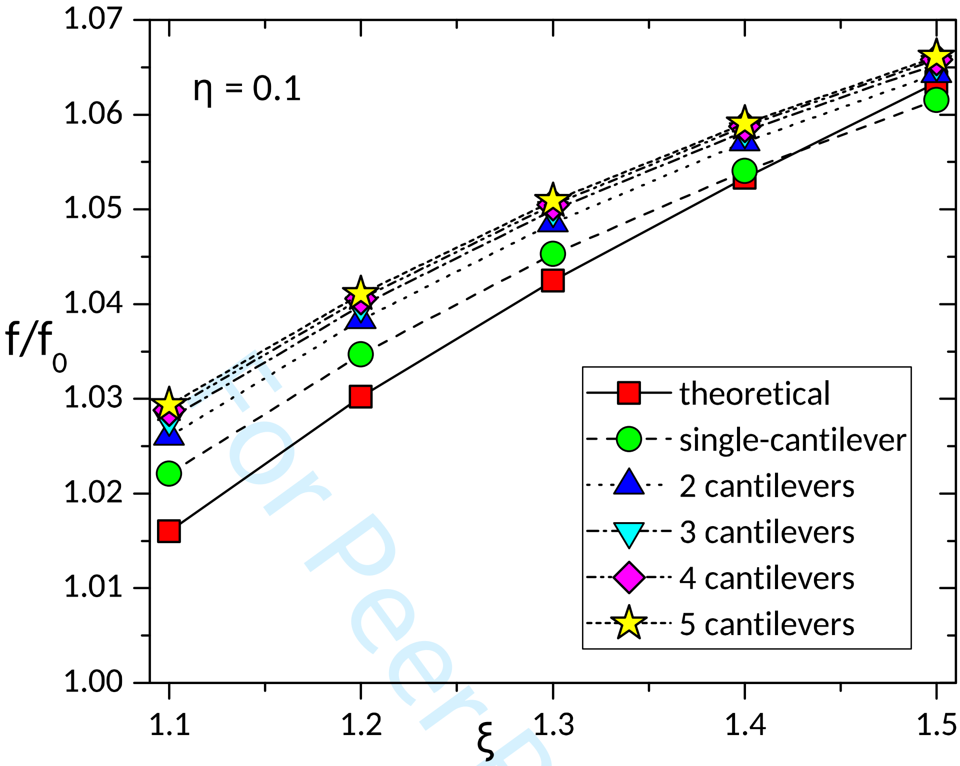

Figure 4: Frequency of a single cantilever in an array of several cantilevers. For $\xi \geq 1.2$, the difference of frequencies of a cantilever in a 2- and 3-cantilever system (blue triangles and aqua inverted triangles) is negligible. The parameters here are same as those used in Fig. 2 where $f_0 = 26.83$ kHz using $\eta = l_0 / L = 0.1$.

4. SEMI-EMPIRICAL MECHANICAL COUPLING STRENGTH

The coupling stiffness between two subsequent cantilevers is the key factor determining the effectiveness of indirect excitation. Via the overhang, the original frequency (ω_A and ω_B) of every cantilever is changed and the two hybrid modes exist (Novotny, 2010)

$$\omega_{\pm}^2 = \frac{1}{2}\left[\omega_A^2 + \omega_B^2 \pm \sqrt{\left(\omega_A^2 - \omega_B^2\right)^2 + 4\Gamma^2 \omega_A \omega_B}\right], \tag{9}$$

where Γ is the anticrossing between ω_+ and ω_- and $\Gamma \propto \kappa$, the coupling strength between two oscillators. For $\omega_A = \omega_B = \omega_0$, one has $\kappa = \frac{k_c}{\omega_0} = \frac{1}{2}\frac{\omega_+^2 - \omega_-^2}{\omega_-^2} = \frac{\Gamma}{\omega_0 - \Gamma} \simeq \frac{\Gamma}{\omega_0}$, and Γ is frequently called the coupling stiffness.

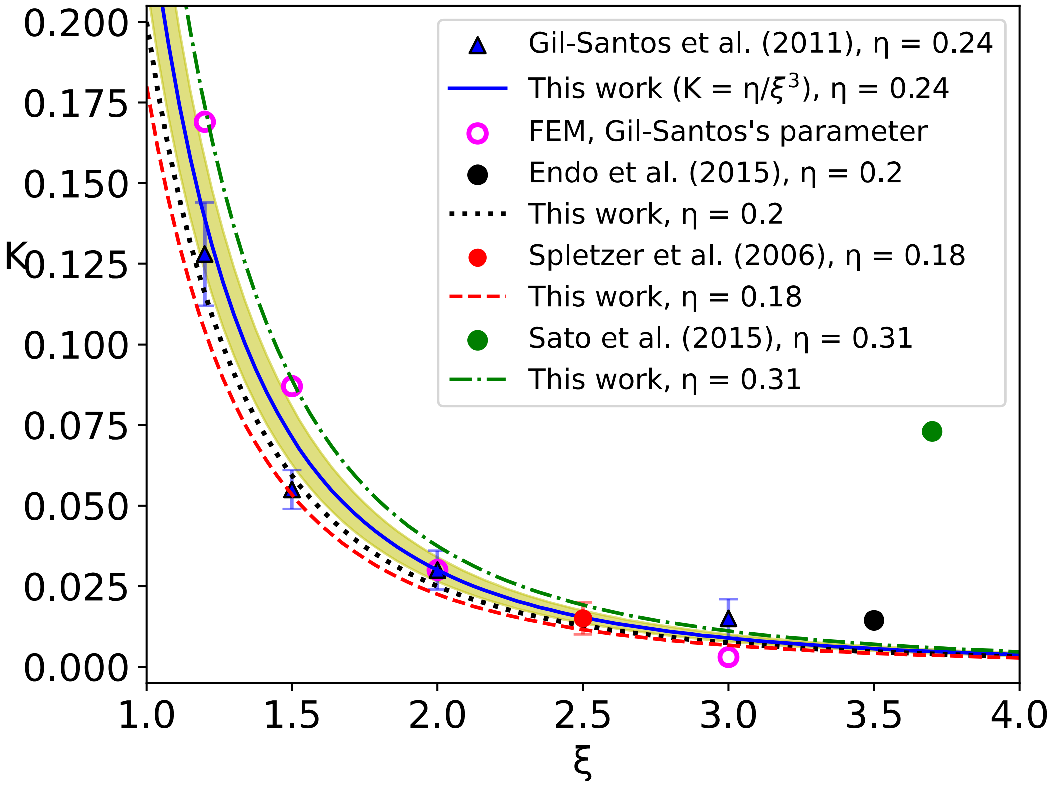

Figure 5: Normalized coupling strength, $\kappa(\eta,\xi) = k_c / \omega_0 = \eta / \xi^3$, in Eq. (10) for $\eta = 0.24$ (black solid lines), 0.2 (blue dotted line), and 0.18 (red dashed line) and experimental values from other groups: blue triangles—the results of Gil-Santos et al., (2011); red circles—the result of Spletzer et al., (2006); black circle—the results of Endo et al., (2015); green circle—the result of Sato et al., (2003) and Chen et al., (2008). The error bars are extracted from the corresponding papers. For $\kappa \sim 10^{-2}$ in Ref. (Spletzer et al., 2006), $\kappa = 0.015$ is selected with a deviation of 0.005. For Ref. (Gil-Santos et al., 2011): magenta circles—the FEM results and yellow shadow—Eq. (10) with $\eta = 0.24 \pm 0.03$.

The value of this coupling is usually deduced to fit with the first two frequencies in experiments. Gil-Santos et al., (2011) suggested that $\kappa_G \propto Ae^{-(\xi-1)/l_0}$, where $\xi - 1$ is the gap between cantilevers; however, this formula involves an unknown parameter A skips the role of the cantilever width and length.

Here, we propose a semi-empirical coupling strength that does not contain any parameters but the reduced dimensions of the overhang, which writes

$$\kappa(\eta,\xi)=\frac{\eta}{\xi^{3}}. \tag{10}$$

Certainly, κ is proportional to the overhang length (η) and diminishes with the increasing gap between subsequent cantilevers ($\xi-1$). Furthermore, it satisfies $\underset{\eta\to 0 \text{ or } \xi-1 ? 0}{\kappa \to 0}$ and $\underset{\eta\to 1}{\kappa\to 1}$, and is presented in Fig. 5 (solid lines). One could rewrite κ as $\kappa(\eta,\xi)=\eta/(\xi-1)^{3}=\eta/p^{3}$ where p is the gap between cantilevers (Gil-Santos et al., 2011); however, this skips the contribution of the cantilever width on the coupling. Experimental values from Gil-Santos et al. (Gil-Santos et al., 2011) (blue triangles), Spletzer et al. (Spletzer et al., 2006) (red circles), Endo et al. (Endo et al., 2015) (black circle), and Sato et al. (Sato et al., 2003) (green circle) have been presented. The error bars when available are also plotted. For Ref. (Spletzer et al., 2006) which used $\kappa \sim 10^{-2}$, we chose $\kappa = 0.015 \pm 0.005$ [see Table 2]. It could be seen that the proposed κ, although very simple, fits well with the experimental values.

Table 2: Coupling strength from experimental parameters, FEM simulations, and semi-empirical formula.

	Cantilever[a]		Overhang			l_0/L	w_0/w	coupling strength (κ)		
Dimensions	L	w	l_0	gap	w_0	η	ξ	experimental	FEM	Eq. (10)
Gil-Santos et al., (2011)	33	10	8	20	30	0.24	3	0.015±0.006	0.003	0.008
				10	20		2	0.030±0.006	0.03	0.03
				5	15		1.5	0.055±0.006	0.087	0.071
				2	12		1.2	0.128±0.016	0.169	0.138
Spletzer et al., (2006)	500	100	90		250	0.18	2.5	0.015±0.005	0.0116	0.0115
Endo et al., (2015)	500	100	100	250	350	0.2	3.5	0.0144	0.0056	0.0046
Sato et al., (2003), Chen et al., (2008)	73.5[b]	15	100		350	0.31	3.7	0.0735	0.0194	0.0062

[a] Dimensions in µm.

[b] An average value from two cantilever lengths.

In fact, the coupling is also dependent on the cantilever thickness and the materials made of the cantilever, i.e. the greater the Young's modulus E is, the higher the coupling is. Therefore, the experimental results could be highly deviated from the semi-empirical value, as shown by green circle for Refs. (Sato et al., 2003) and (Chen et al., 2008) versus the green dash-dotted line. We could write a more general form for κ as $\kappa = A(E)\eta / \xi^3$. Nevertheless, in the case of silicon and silicon nitride cantilever, the simple form of Eq. (10) still describes well the coupling, i.e. $A(E)=1$ was used. Using the FEM simulation (magenta circles) to check the experimental results, we could see that there is a significant deviation of κ for small overhang lengths, e.g. $\xi = 1.2$. This arises from the deviation in the overhang length in fabrication, $l_0 = 8 \pm 1\ \mu m$, which gives rise to $\eta = 0.24 \pm 0.03$ (yellow shadow in the figure). For greater overhang lengths, $\xi = 1.5 - 2.5$, the formula agrees well with both the experimental and FEM results.

5. CONCLUSION

In summary, we have figured out an analytical formula for the characteristic frequency of overhang- and T-shaped cantilevers. The formula involves a symmetric term of cantilever (Gil-Santos et al., 2011) and overhang lengths in addition to the empirical term of a rectangular cantilever. FEM simulation has been used to confirm the accuracy of the analytical equation. A deviation below 3% is obtained for the overhang that 3-fold wider than the cantilever width. The analytical procedure could be applied for doubly clamped cantilever with various width geometries such as tapered, anti-tapered, or normal beam with symmetrical attachment in the middle (Bereyhi et al., 2019; N. D. Vy, Cuong, & Hoang, 2018). Especially, a semi-empirical formula for the coupling strength between cantilevers in an array has been presented which shows a good agreement with the values from experiments of other research groups.

ACKNOWLEDGEMENTS

Authors are thankful to Dr. Hien Duy Tong (Nanosens Research B.V., The Netherlands) for fabrication of cantilevers. N.D. Vy is thankful to the Van Lang University. This research is funded by Vietnam National Foundation for Science and Technology Development (NAFOSTED) under grant number 103.01-2019.345.

AUTHOR DECLARATIONS

Conflict of Interest

The authors have no conflicts to disclose.

DATA AVAILABILITY

The data that support the findings of this study are available from the corresponding author upon reasonable request.

RERERENCES

Adiga, V. P., Sumant, A. V., Suresh, S., Gudeman, C., Auciello, O., Carlisle, J. A., & Carpick, R. W. (2009). Mechanical stiffness and dissipation in ultrananocrystalline diamond microresonators. *Physical Review B, 79*(24), 245403. doi:10.1103/PhysRevB.79.245403

Bereyhi, M. J., Beccari, A., Fedorov, S. A., Ghadimi, A. H., Schilling, R., Wilson, D. J., . . . Kippenberg, T. J. (2019). Clamp-Tapering Increases the Quality Factor of Stressed Nanobeams. *Nano Letters, 19*(4), 2329-2333. doi:10.1021/acs.nanolett.8b04942

Blevins, R. D. (2015). *Formulas for dynamics, acoustics and vibration*: John Wiley & Sons.

Cai, G., Zhang, R., Wang, Z., Zhao, L., & Wu, W. (2013, 3-6 Nov. 2013). *Net-overhang coupled microcantilevers for sensitive mass detection.* Paper presented at the SENSORS, 2013 IEEE.

Chen, Q., Huang, L., & Lai, Y.-C. (2008). Chaos-induced intrinsic localized modes in coupled microcantilever arrays. *Applied Physics Letters, 92*(24), 241914. doi:10.1063/1.2946494

Chopard, T., Lacour, V., & Leblois, T. (2014). GaAs Coupled Micro Resonators with Enhanced Sensitive Mass Detection. *Sensors, 14*(12). doi:10.3390/s141222785

Endo, D., Yabuno, H., Higashino, K., Yamamoto, Y., & Matsumoto, S. (2015). Self-excited coupled-microcantilevers for mass sensing. *Applied Physics Letters, 106*(22), 223105. doi:10.1063/1.4921082

Gil-Santos, E., Ramos, D., Pini, V., Calleja, M., & Tamayo, J. (2011). Exponential tuning of the coupling constant of coupled microcantilevers by modifying their separation. *Applied Physics Letters, 98*(12), 123108. doi:10.1063/1.3569588

Guillon, S., Saya, D., Mazenq, L., Perisanu, S., Vincent, P., Lazarus, A., . . . Nicu, L. (2011). Effect of non-ideal clamping shape on the resonance frequencies of silicon nanocantilevers. *Nanotechnology, 22*(24), 245501. doi:10.1088/0957-4484/22/24/245501

Hoang, C. M., Vy, N. D., Dat, L. T., & Iida, T. (2017). Enhancing amplitudes of higher-order eigenmodes of atomic force microscope cantilevers by laser for better mass sensing. *Japanese Journal of Applied Physics, 56*(6S1), 06GK05. doi:10.7567/jjap.56.06gk05

Huber, F., Lang, H. P., Zhang, J., Rimoldi, D., & Gerber, C. (2015). Nanosensors for cancer detection. *Swiss medical weekly, 145*.

Kim, S., Lee, D., Liu, X., Van Neste, C., Jeon, S., & Thundat, T. (2013). Molecular recognition using receptor-free nanomechanical infrared spectroscopy based on a quantum cascade laser. *Scientific Reports, 3*(1), 1111. doi:10.1038/srep01111

Kimura, M., & Hikihara, T. (2009). Capture and release of traveling intrinsic localized mode in coupled cantilever array. *Chaos: An Interdisciplinary Journal of Nonlinear Science, 19*(1), 013138. doi:10.1063/1.3097068

Krylov, S., Lulinsky, S., Ilic, B. R., & Schneider, I. (2014). Collective dynamics and pattern switching in an array of parametrically excited micro cantilevers interacting through fringing electrostatic fields. *Applied Physics Letters, 105*(7), 071909. doi:10.1063/1.4893593

McKendry, R., Zhang, J., Arntz, Y., Strunz, T., Hegner, M., Lang, H. P., . . . Gerber, C. (2002). Multiple label-free biodetection and quantitative DNA-binding assays on a nanomechanical cantilever array. *Proceedings of the National Academy of Sciences, 99*(15), 9783. doi:10.1073/pnas.152330199

Meirovitch, L. (1967). *Analytical methods in vibrations*: Macmillan.

Mukhopadhyay, R., Sumbayev, V. V., Lorentzen, M., Kjems, J., Andreasen, P. A., & Besenbacher, F. (2005). Cantilever Sensor for Nanomechanical Detection of Specific Protein Conformations. *Nano Letters, 5*(12), 2385-2388. doi:10.1021/nl051449z

Napoli, M., Wenhua, Z., Turner, K., & Bamieh, B. (2005). Characterization of electrostatically coupled microcantilevers. *Journal of Microelectromechanical Systems, 14*(2), 295-304. doi:10.1109/JMEMS.2004.839349

Novotny, L. (2010). Strong coupling, energy splitting, and level crossings: A classical perspective. *American Journal of Physics, 78*(11), 1199-1202. doi:10.1119/1.3471177

Payam, A. F., Trewby, W., & Voïtchovsky, K. (2018). Determining the spring constant of arbitrarily shaped cantilevers in viscous environments. *Applied Physics Letters, 112*(8), 083101. doi:10.1063/1.5009071

Plaza, J. A., Zinoviev, K., Villanueva, G., Álvarez, M., Tamayo, J., Domínguez, C., & Lechuga, L. M. (2006). T-shaped microcantilever sensor with reduced deflection offset. *Applied Physics Letters, 89*(9), 094109. doi:10.1063/1.2345234

Sato, M., Hubbard, B. E., & Sievers, A. J. (2006). Colloquium: Nonlinear energy localization and its manipulation in micromechanical oscillator arrays. *Reviews of Modern Physics, 78*(1), 137-157. doi:10.1103/RevModPhys.78.137

Sato, M., Hubbard, B. E., Sievers, A. J., Ilic, B., Czaplewski, D. A., & Craighead, H. G. (2003). Observation of Locked Intrinsic Localized Vibrational Modes in a Micromechanical Oscillator Array. *Physical Review Letters, 90*(4), 044102. doi:10.1103/PhysRevLett.90.044102

Singh, S. S., Pal, P., & Pandey, A. K. (2015). Pull-in analysis of non-uniform microcantilever beams under large deflection. *Journal of Applied Physics, 118*(20), 204303. doi:10.1063/1.4936321

Spletzer, M., Raman, A., Wu, A. Q., Xu, X., & Reifenberger, R. (2006). Ultrasensitive mass sensing using mode localization in coupled microcantilevers. *Applied Physics Letters, 88*(25), 254102. doi:10.1063/1.2216889

Sposito, A. J., Kurdekar, A., Zhao, J., & Hewlett, I. (2018). Application of nanotechnology in biosensors for enhancing pathogen detection. *WIREs Nanomedicine and Nanobiotechnology, 10*(5), e1512. doi:https://doi.org/10.1002/wnan.1512

Tamayo, J., Ramos, D., Mertens, J., & Calleja, M. (2006). Effect of the adsorbate stiffness on the resonance response of microcantilever sensors. *Applied Physics Letters, 89*(22), 224104. doi:10.1063/1.2388925

Timoshenko, S. P., & Young, D. H. (1937). *Engineering mechanics statics*. Retrieved from

Toda, M., Inomata, N., Ono, T., & Voiculescu, I. (2017). Cantilever beam temperature sensors for biological applications. *IEEJ Transactions on Electrical and Electronic Engineering, 12*(2), 153-160. doi:https://doi.org/10.1002/tee.22360

Vy, N. D., Cuong, N. V., & Hoang, C. M. (2018). A Mechanical Beam Resonator Engineered at Nanoscale for Ultralow Thermoelastic Damping. *Journal of Mechanics, 35*(3), 351-358. doi:10.1017/jmech.2018.22

Vy, N. D., Tri Dat, L., & Iida, T. (2016). Cancelation of thermally induced frequency shifts in bimaterial cantilevers by nonlinear optomechanical interactions. *Applied Physics Letters, 109*(5), 054102. doi:10.1063/1.4960380

Xu, L.-C., & Siedlecki, C. A. (2009). Atomic Force Microscopy Studies of the Initial Interactions between Fibrinogen and Surfaces. *Langmuir, 25*(6), 3675-3681. doi:10.1021/la803258h

Yabuno, H., Seo, Y., & Kuroda, M. (2013). Self-excited coupled cantilevers for mass sensing in viscous measurement environments. *Applied Physics Letters, 103*(6), 063104. doi:10.1063/1.4817979